ELSEVIER

Applied Catalysis A: General 230 (2002) 281–291

APPLIED CATALYSIS A: GENERAL

www.elsevier.com/locate/apcata

Layered double hydroxide-derived vanadium catalysts for oxidative dehydrogenation of propane Influence of interlayer-doping versus layer-doping

R. Dula [a], K. Wcisło [a], J. Stoch [a], B. Grzybowska [a], E.M. Serwicka [a,*], F. Kooli [b], K. Bahranowski [c], A. Gaweł [c]

[a] *Institute of Catalysis and Surface Chemistry, Polish Academy of Sciences, ul. Niezapominajek 8, 30-239 Cracow Poland*
[b] *National Institute for Research in Inorganic Materials, Namiki 1-1, Tsukuba, Ibaraki 305, Japan*
[c] *Faculty of Geology, Geophysics and Environmental Protection, Academy of Mining and Metallurgy, al. Mickiewicza 30, 30-059 Cracow, Poland*

Received 11 April 2001; received in revised form 14 January 2002; accepted 14 January 2002

Abstract

Mixed-oxide vanadium catalysts for oxidative dehydrogenation (ODH) of propane have been prepared by thermal decomposition of Mg, Al-layered double hydroxides (LDHs) containing vanadium either in the brucite layer or in the interlayer. The materials have been characterised by XRD, ICP-AES chemical analysis, XPS, BET and ESR. The catalytic performance of the samples depended on the manner of incorporation of the vanadium into the LDH structure. The sample obtained from interlayer-doped precursor was more active and more selective than mixed oxides obtained from layer-doped LDHs. The difference in the catalytic properties was attributed to the different magnesium vanadates nucleating in the calcined samples, the pyrovanadate formed from the interlayer-doped LDH giving better performance than *ortho*-vanadate crystallising from the layer-doped precursor. It has been suggested that one of the factors contributing to the difference in the behaviour of both types of catalysts might be the difference in the covalency of V–O in-plane bonds around the reduced V centres.

Keywords: Hydrotalcites; Layered double hydroxides; Oxidative dehydrogenation; V-Mg-O mixed oxides

1. Introduction

Oxidative dehydrogenation (ODH) of light alkanes is an attractive route to convert low cost chemicals into more valuable unsaturated hydrocarbons. Catalysts containing vanadium as the main component are among the most extensively investigated for ODH processes [1]. In particular, much attention has been given to V-Mg-O mixed system, which proved as one of the most active and selective in the ODH of short-chain paraffins to corresponding olefins [2–13]. The catalysts are usually prepared by impregnation of a magnesium-containing support (e.g. MgO, $Mg(OH)_2$) with a vanadium precursor solution, followed by calcination at elevated temperature, or by solid state reaction between magnesia and vanadia. Their activities and selectivities depend on the V/Mg ratio and are usually related to the oxide phase composition, although contradictory conclusions have been drawn as to the exact nature of the active phase. While Kung

* Corresponding author. Tel.: +48-12-425-2814; fax: +48-12-425-1923.
E-mail address: ncserwic@cyf-kr.edu.pl (E.M. Serwicka).

0926-860X/02/$ – see front matter
PII: S0926-860X(02)00041-8

and co-workers [2] attributed the catalyst activity to the presence of magnesium *ortho*-vanadate $Mg_3V_2O_8$, the group of Volta and co-workers [3] argued that magnesium pyrovanadate (α-$Mg_2V_2O_7$) was the key component responsible for the good performance of V-Mg-O catalysts. Gao et al. [6] reported that the performance of pure magnesium vanadates could be significantly affected by the coexistence of other phase.

It has been indicated that the appearance and the relative proportions of different phases in the Mg-V-O system depend to a large extent on the method of catalyst preparation [1,5]. This prompted some of us to employ synthetic procedures used for the preparation of layered double hydroxides (LDHs) to obtain the precursors of the potentially active mixed oxide system [14]. LDHs, known also as hydrotalcites or anionic clays, consist of brucite [$Mg(OH)_2$]-like layers with part of the divalent cations substituted by the trivalent ones. As a result, the layers acquire excess positive charge which is compensated by the incorporation of hydrated anions into the interlayer space. The general formula may be thus, given as $[M(II)_{1-x}M(III)_x(OH)_2]A_{x/n}{}^{n-} \cdot mH_2O$, where M(II) and M(III) are the layer forming cations and A^{n-} is the interlayer anion. Due to the homogeneous distribution of M(II) and M(III) in the LDH framework and to the layered structure, these materials yield upon thermal decomposition mixed oxides of both cations with unique surface and catalytic properties [15]. If the interlayer anion is an oxometalate, then yet another metal oxide component may be added to the mixed oxides obtained by calcination of the LDH matrix. We have shown [14] that the use of Mg,Al-LDH with decavanadate anions in the interlayer as a mixed oxide phase precursor produced a catalyst whose performance in the ODH of propane was, depending on temperature of the reaction, comparable or slightly better than the V-Mg-O catalyst of optimum characteristics obtained by the impregnation method of Chaar et al. [2]. Since the report by Rives et al. [16] it is known that vanadium can be also incorporated into the brucite layer, as V(III). Subsequent reports [17,18] indicated that there is a substantial difference in the nature of magnesium vanadates formed upon calcination, depending on the location of the vanadium dopant in the LDH precursor. While the interlayer-doped material led to the crystallisation of pyrovanadate and *meta*-vanadate phases, the layer-doped precursors produced invariably the *ortho*-vanadate phase.

In view of the former discussion on the role of different magnesium vanadates in the ODH of propane, it seemed of interest to check on the influence of layer-doping versus interlayer-doping with vanadium on the catalytic properties of mixed oxide phases obtained upon calcination of corresponding LDH precursors.

2. Experimental

2.1. Materials

The starting material to obtain the interlayer-doped LDH was an Mg,Al-LDH with Mg/Al = 2 prepared by a standard co-precipitation procedure. 0.06 M of $Mg(NO_3)_2 \cdot 6H_2O$ and 0.03 M of $Al(NO_3)_2 \cdot 9H_2O$ were dissolved in 50 ml distilled water and added dropwise to 100 ml of distilled water at pH 10, controlled by dropwise addition of 2 M NaOH. The suspension was magnetically stirred overnight at 328 K, the precipitate centrifuged, washed several times with distilled water and left in the form of suspension used subsequently in the exchange experiments with a solution of decavanadate anions. The parent sample is referred to as $MgAlNO_3$-LDH. The decavanadate solution was prepared by dissolving 0.05 M of $NaVO_3$ in 150 ml distilled water at pH 4.5, which favours formation of $V_{10}O_{28}{}^{6-}$ species [19]. Ion exchange was carried out by a dropwise addition of the decavanadate solution to the $MgAlNO_3$-LDH suspension, at 328 K. The pH was kept at 4.5 by a dropwise addition of 0.5 M HNO_3. The exchange product, referred to as $MgAlV_{10}O_{28}$-LDH, was washed with distilled water and dried at 323 K.

The layer-doped LDHs were prepared as carbonate forms with Mg/(V + Al) = 3 and Al/V = y (y = 0.0, 2.0), following the method described by Kooli et al. [18]. They were obtained by a dropwise addition of an appropriate amount of aqueous solutions of $MgCl_2 \cdot 6H_2O$, $AlCl_3 \cdot 6H_2O$ and VCl_3 to sodium carbonate solution at a constant pH = 9 controlled by a dropwise addition of 2 M NaOH. The solid products were washed with hot water and treated hydrothermally at 393 K for 48 h, then filtered and dried. The products are referred to as $MgAl_y$ VCO_3-LDH.

Prior to catalytic experiments the LDH precursors were converted to mixed oxide (MO) phases by 24 h calcination in air at 823 K. The calcined materials are referred to as $MgAlV_{10}O_{28}$-MO and $MgAl_yVCO_3$-MO.

2.2. Methods

Samples were characterised with XRD, XPS, BET, chemical analysis and ESR. The XRD patterns were obtained with a DRON-3 diffractometer using Ni-filtered Cu Kα radiation. The XPS spectra were obtained with a VG-ESCA 3 spectrometer using Al $K\alpha_{1,2}$ radiation (1486.6 eV). Data processing consisted of calibration of the peak position against the C 1s line from adventitious surface carbon deposit (284.8 eV), removal of background and $K\alpha_{3,4}$ peaks, and fitting the resulting spectra with single peaks or multiplets using a Voigt function with 30% Lorenzian character. The relative element content (N_A) was calculated from the following formula [20]:

$$N_A = FI_A E_A^{0.25} \sigma_A^{-1} \exp(d_C \lambda_{CA}^{-1})$$

where F contains all instrumental factors and is assumed to be constant for all measurements, I_A is the integrated peak area, E_A the kinetic energy of electrons, σ_A the atomic cross-section for the ionisation of the A-level, d_C the thickness of carbon deposit, and λ_{CA} is the A-level electrons' inelastic mean free path in the adventitious carbon layer. The BET specific surface area of the samples was determined from argon adsorption at 77 K, after outgassing at 473 K. Chemical analysis was carried out on an ICP-AES Plasma 40 Perkin-Elmer spectrometer, after dissolution of the samples in nitric acid. The ESR spectra were recorded at room temperature and at 77 K with an X-band SE/X (Technical University Wrocław) spectrometer. ESR parameters were determined from the computer simulations by using the simulation programs SIMAX and COMBI, kindly made available by Dr. J.C. Conesa from Instituto de Catalisis y Petrolooquimica CSIC, Madrid, Spain. SIMAX is applicable for $S = 1/2$ systems with axial symmetry and allows for hyperfine interaction with one atom in the paramagnetic species. Of this atom, up to three isotopes are allowed to exist, and of these isotopes at most two may have non-zero nuclear spin. SIMAX takes also into account the nuclear quadrupole interactions and "forbidden" hyperfine transitions induced by it. The appropriate resonance condition is computed using the second-order perturbation formulas [21,22], with the transition probability including the correction of Aasa and Vangard [23]. COMBI enables to obtain linear combinations of up to four SIMAX simulations. In some cases, in order to enhance weak ESR spectra in the oxidised materials, the samples were reduced at room temperature with hydrogen atoms produced by hydrogen spillover. In a typical experiment, 5 wt.% of the Pd/Al_2O_3 (Fluka, puriss.) catalyst was mixed with an LDH sample and exposed to 50 Torr hydrogen over the period of 30–90 min. As pointed out by Serwicka [24] such an experiment allows reduced species to be produced without any significant distortion of the surrounding matrix, in particular with no extraction of lattice oxygens.

2.3. Catalysis

The ODH of propane was carried out under atmospheric pressure in the temperature range 573–803 K, in a fixed bed flow reactor, with on-line GC product analysis. The reactor (120 mm long, i.d. 13 mm) was made of stainless steel. The thermocouple for the temperature measurement was placed co-axially in the catalyst bed. Propane, CO, CO_2 and water were the only reaction products. The catalyst volume was 0.5 cm^3 (ca. 0.3 g), particle size 0.2–0.5 mm, the contact time (catalyst volume/total flow) 1 s. The reaction mixture contained 17 vol.% of propane in air. A blank test without a catalyst showed less than 1% conversion of propane up to 773 K (flow rate 30 ml/min).

3. Results and discussion

3.1. Characterisation of the catalysts

The powder XRD patterns of the V-containing LDHs are presented in Fig. 1. The XRD diagram of the interlayer-doped $MgAlV_{10}O_{28}$-LDH consists of a broad reflection at ca. 10.0 Å, followed by sharp reflections at 5.83 and 3.91 Å as well as several less intense peaks (Fig. 1a). The sharp peaks can be indexed as (0 0 6) and (0 0 9) of the decavanadate-exchanged LDH structure [25–29] for which the (0 0 3) reflection,

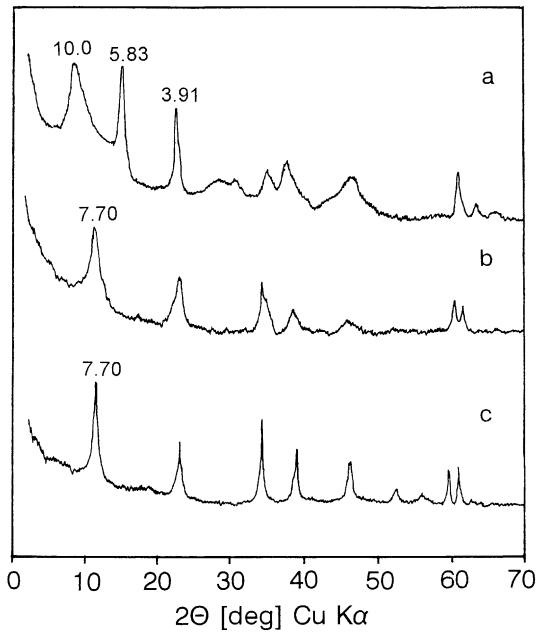

Fig. 1. XRD patterns of starting LDH materials: (a) $MgAlV_{10}O_{28}$-LDH, (b) $MgAl_{2.0}VCO_3$-LDH, (c) $MgAl_{0.0}VCO_3$-LDH.

expected at 11.70 Å, is obscured by the low angle broad peak. The origin of the latter has been frequently discussed over the years. It has been assigned either to a polyoxometelate salt impurity formed by reaction of the cations from the partially dissolved brucite layer with the polyoxoanions used for intercalation [26] or to a defect LDH structure resulting from acid damage [29]. The XRD patterns of layer-doped materials (Fig. 1b and c) are consistent with the carbonate-containing LDH structure ($d_{003} = 7.70$ Å) and analogous to those described by Kooli et al. [18].

The formulas of the samples calculated from the elemental chemical analysis are given in Table 1. In all V-doped materials, the experimental $Mg/\sum M(III)$ ratio is lower than the nominal one. A similar phenomenon has been observed previously [18]. In the case of the layer-doped samples, the authors interpreted the effect as arising from the differences in the pH values required to precipitate the cations involved in the synthesis. In consequence, at the pH = 9, a preferential precipitation of cations forming less soluble hydroxides, i.e. Al(III) and V(III), occurs, the conditions for the precipitation of Mg(II) being less favourable. In the case of interlayer-doped LDH, the deficit of magnesium is caused by its partial dissolution from the $MgAlNO_3$ matrix during exchange experiment carried out in the acidic medium (pH = 4.5).

Calcination of the vanadium-containing LDHs at 823 K results in mixed oxide materials whose XRD diagrams are presented in Fig. 2. The pattern of the $MgAlV_{10}O_{28}$-MO sample (Fig. 2a) resembles the spectrum of a V/MgO catalyst containing 38 wt.% vanadium, prepared by impregnation by Volta and co-workers [3]. It may be interpreted as a superposition of diffraction lines belonging to MgO and some magnesium vanadate phases. The MgO lines at $2\theta \approx 64^\circ$ and $2\theta \approx 44^\circ$, which may be assigned to the most intense (2 0 0) and (2 2 0) reflections, are slightly shifted towards higher angles with respect to the pure magnesia. This is indicative of the formation of a defect MgO structure, usually described as magnesia-alumina solid solution [28]. The other lines have been assigned previously [3] to α-$Mg_2V_2O_7$ magnesium pyrovanadate phase. Indeed, the comparison with the ASTM file of α-$Mg_2V_2O_7$ (31-0816) shows that the peak around $2\theta \approx 18^\circ$, peaks around $2\theta \approx 30^\circ$ and the envelope around $2\theta \approx 37^\circ$ which contains also a contribution from an MgO peak, are consistent with such an assignment. A high background in the area $10^\circ < 2\theta < 40^\circ$ suggests the presence of highly disordered amorphous phase. After additional calcination at 923 K, a well

Table 1
Composition of LDH samples from chemical analysis

Sample	Formula	$Mg/\sum M(III)$[a]	V (wt.%) in the mixed oxide phase
$MgAlV_{10}O_{28}$-LDH	$[Mg_{0.61}Al_{0.39}(OH)_2](V_{10}O_{28})_{0.065}\cdot 0.9H_2O$	1.54 (2)	32.0
$MgAl_{2.0}VCO_3$-LDH	$[Mg_{0.68}Al_{0.21}V_{0.11}(OH)_2](CO_3)_{0.16}\cdot 0.6H_2O$	2.12 (3)	11.7
$MgAl_{0.0}VCO_3$-LDH	$[Mg_{0.62}V_{0.38}(OH)_2](CO_3)_{0.19}\cdot 0.7H_2O$	1.63 (3)	32.5

[a] Expected values in parentheses.

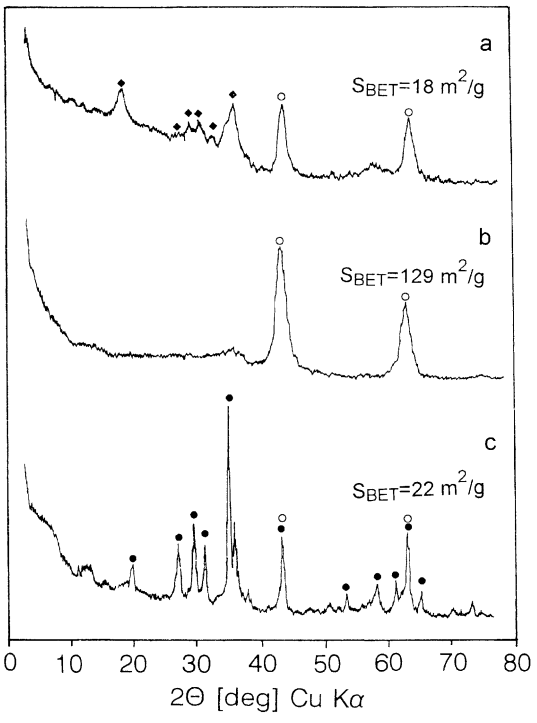

Fig. 2. XRD patterns of calcined LDH precursors: (a) $MgAlV_{10}O_{28}$-MO, (b) $MgAl_{2.0}VCO_3$-MO, (c) $MgAl_{0.0}VCO_3$-MO. (◆) α-$Mg_2V_2O_7$, (○) Al-doped MgO, (●) $Mg_3V_2O_8$.

crystalline α-$Mg_2V_2O_7$ phase is formed. Sample $MgAl_{2.0}VCO_3$-MO shows only peaks characteristic of the Al-doped MgO, while vanadium-containing phase remains amorphous (Fig. 2b). No change is observed in the XRD diagram of this material even after the additional thermal treatment at 923 K. The XRD of $MgAl_{0.0}VCO_3$-MO gives a well resolved pattern already after calcination at 823 K, typical of magnesium *ortho*-vanadate $Mg_3V_2O_8$ [30] and MgO. Crystallinity of this sample is much better than that of $MgAlV_{10}O_{28}$-MO (Fig. 2a). This, however, is not reflected in the specific surface areas of the materials, which are 18 and 22 m^2/g for $MgAlV_{10}O_{28}$-MO and $MgAl_{2.0}VCO_3$-MO, respectively. Also the surface morphology of the samples examined with SEM (not shown) is similar in both cases and shows crystallites of order of 0.1 μm. Thus, the poorer crystallinity of $MgAlV_{10}O_{28}$-MO is not reflected in the appearance of the individual grains. The weight percent of vanadium in the calcined materials is given in Table 1.

The formation of magnesium pyrovanadate from the $MgAlV_{10}O_{28}$-LDH precursor and magnesium *ortho*-vanadate from the $MgAl_{0.0}VCO_3$-LDH sample may be intuitively understood when one considers the nature of V species present in the precursors and in the final decomposition products. In the first case, vanadium is present in the LDH as polymeric decavanadate species, which on heating partially de- and re-polymerise and provide chains of reactive $(VO_3)_n^{n-}$ ready to form α-$Mg_2V_2O_7$ with its dimeric $(V_2O_7)^{4-}$ units [31]. In the second case, the vanadium centres are dispersed among magnesium ions surrounded by closely packed hydroxyl groups of the brucite layer and the transformation to nearly cubic closest packing of oxygen atom layers with the Mg ions retaining their octahedral surrounding and the V ions occupying isolated tetrahedral positions characteristic of the $Mg_3V_2O_8$ structure [30], seems straightforward.

The XPS analysis has been carried out in order to assess the density of V centres at the surface of calcined samples and the results are presented in Table 2. In all cases, surface enrichment in magnesium is observed, in agreement with previous findings for V-Mg-O catalysts [3,6]. In samples $MgAlV_{10}O_{28}$-MO and $MgAl_{0.0}VCO_3$-MO, the density of surface V centres measured with respect to the surface oxygens is very similar and about five times higher than in the $MgAl_{2.0}VCO_3$-MO catalyst.

ESR investigation of these materials, described in detail elsewhere [32], undertaken in order to monitor the changes in the LDH precursor upon thermal decomposition, demonstrated that in the calcined samples vanadium centres of different electronic structure are formed, depending on the location of vanadium within the LDH precursor. Table 3 shows the ESR parameters of V(IV) defects present in mixed oxide materials obtained by calcination at 773 K. The

Table 2
BET specific surface areas and XPS determined surface V content (atomic ratios) in calcined V-doped LDHs

Sample	S_{BET} (m^2/g)	V/Mg[a]	V/O
$MgAlV_{10}O_{28}$-MO	18	0.86 (1.06)	0.18
$MgAl_{2.0}VCO_3$-MO	129	0.11 (0.16)	0.04
$MgAl_{0.0}VCO_3$-MO	22	0.4 (0.61)	0.19

[a] Bulk values in parentheses.

Table 3
ESR parameters of V(IV) present in the mixed oxide phases obtained by calcination of LDH precursors

Sample	$g_{\parallel}$	$g_{\perp}$	$\lvert A_{\parallel}\rvert$ ($\times 10^4$ cm^{-1})	$\lvert A_{\perp}\rvert$ ($\times 10^4$ cm^{-1})	β_2^2	B
$MgAlV_{10}O_{28}$-MO	1.937	1.968	163.1	52.9	0.82	1.9
$MgAl_{2.0}VCO_3$-MO[a]	1.940	1.960	158.9	56.1	0.77	1.5
$MgAl_{0.0}VCO_3$-MO[a]	1.940	1.973	159.5	55.9	0.78	2.1

[a] ESR parameters determined from signals of samples treated with spilled-over hydrogen (adapted from [32]).

experimentally observed values of $g_{\parallel} < g_{\perp}$ and $|A_{\parallel}| > |A_{\perp}|$ indicate the formation of a vanadyl bond in the vanadium species responsible for the ESR signals [32]. The most important differences concern the β_2^2 parameter, which is the molecular orbital coefficient providing information about the degree of localisation of the unpaired electron on the vanadium d_{xy} orbital, which in turn informs about the extent of the V–O π-covalent bonding in the plane perpendicular to the vanadyl bond. In the case of samples derived from layer-doped precursors β_2^2 is lower than for sample obtained from interlayer-doped LDH. This means that in the former case the extent of the de-localisation of the unpaired electron onto in-plane ligands is higher and the corresponding bonds possess more covalent character than in the material obtained from the decavanadate-exchanged precursor. This finding is in line with the XRD analysis showing the existence of the *ortho*-vanadate phase in the $MgAl_{0.0}VCO_3$-MO sample and the pyrovanadate component in the $MgAlV_{10}O_{28}$-MO material. As pointed out by Volta and co-workers [3] on the basis of the structural considerations supported by the XPS data, the V–O bonding in $Mg_3V_2O_8$ is more covalent than in α-MgV_2O_7. Our ESR observations give further support for the above statement. Table 3 informs also about the value of parameter B, defined as $(g_{\parallel} - g_e)/(g_{\perp} - g_e)$, where g_e is the free electron g value. According to Sharma et al. [33], for a paramagnetic complex in square pyramidal or tetragonally distorted octahedral surrounding B is a sensitive indicator of changes in the local symmetry. If no angular distortion occurs, its increase points to either shortening of the V=O bond or to the elongation of the distance to the in-plane ligands. Comparison of B for $MgAl_{2.0}VCO_3$-MO and $MgAl_{0.0}VCO_3$-MO, both derived from layer-doped precursors but differing by the presence or lack of aluminium, shows that in the former case, B has a lower value. This suggests, that upon incorporation of aluminium changes in the bond length around the V centre occur that may be interpreted as a relative shortening of the in-plane V–O distances or lengthening of V=O bond.

3.2. Catalysis

Results of the ODH of propane over $MgAlV_{10}O_{28}$-MO, $MgAl_{2.0}VCO_3$-MO and $MgAl_{0.0}VCO_3$-MO are presented in Figs. 3–6. Fig. 3 shows the dependence of the propane conversion on the reaction temperature. The $MgAlV_{10}O_{28}$-MO is clearly the most active of all investigated catalysts, while the $MgAl_{2.0}VCO_3$-MO and $MgAl_{0.0}VCO_3$-MO samples prepared from precursors containing vanadium in the brucite layer give poorer performance. Particularly, noteworthy is the much higher activity of the $MgAlV_{10}O_{28}$-MO catalyst with respect to the $MgAl_{0.0}VCO_3$-MO material, containing comparable amount of total vanadium, and possessing similar surface density of V sites and specific surface area. Figs. 4–6 show the temperature dependences of the selectivities to propene, carbon dioxide and carbon monoxide. It is convenient to discuss the observed trends in terms of a parallel-consecutive mechanism typical of selective oxidation reactions of hydrocarbons on oxide catalysts, observed previously on other V-containing materials [3,34–37].

$$\begin{array}{ccc} C_3H_8 & \rightarrow & C_3H_6 \\ \searrow & & \downarrow \\ & CO_2 + CO & \end{array}$$

Analysis of the figures shows differences in the selectivity patterns recorded for samples differing by the manner of V-doping. The selectivity to propene over $MgAlV_{10}O_{28}$-MO, initially at the level of 70–80%, steadily decreases with the increasing temperature, i.e. with the increasing propane conversion (Fig. 4). This is a common feature of many ODH catalysts and is

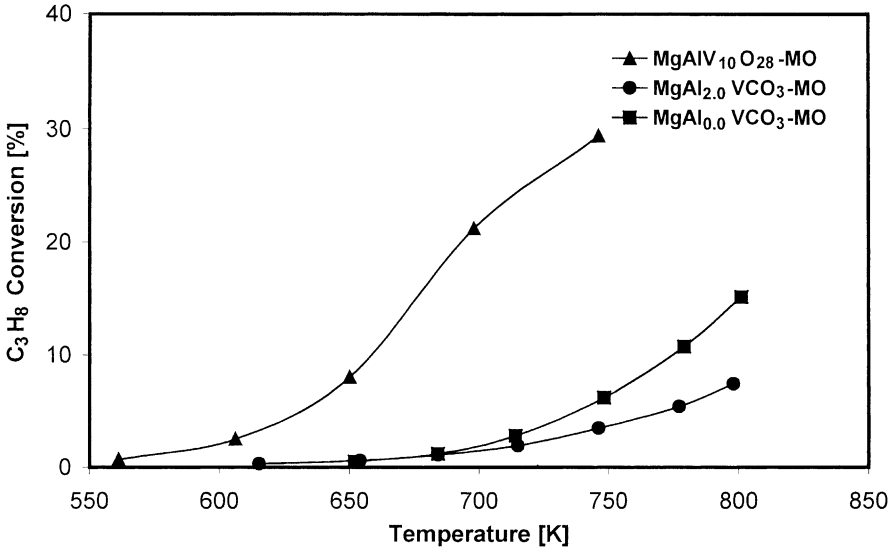

Fig. 3. Temperature dependence of propane conversion.

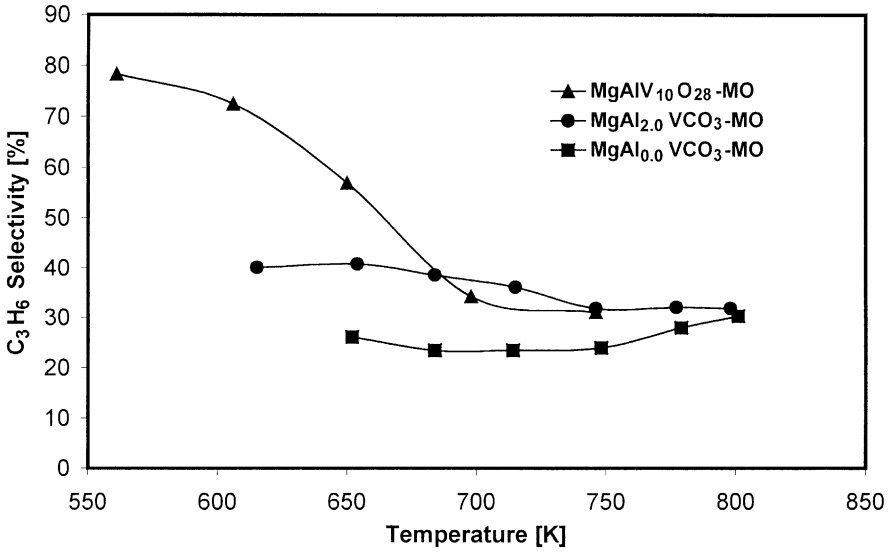

Fig. 4. Temperature dependence of selectivity to propene.

due to the increasing contribution of the total oxidation processes occurring via consecutive propene combustion and parallel propane oxidation. Indeed, on this catalyst, a simultaneous increase of selectivities to CO and CO_2 is observed, that of CO being more distinct than that of CO_2 (Figs. 5 and 6). In consequence, for the temperatures >650 K, the selectivity to CO is higher than that of CO_2. In contrast, the initial selectivity to propene on the $MgAl_{2.0}VCO_3$-MO and the $MgAl_{0.0}VCO_3$-MO materials obtained from layer-doped precursors is much lower, but varies only little with temperature (Fig. 4). Moreover, in both cases, the selectivity to CO_2 is considerably higher than that to CO. It has been repeatedly pointed out that

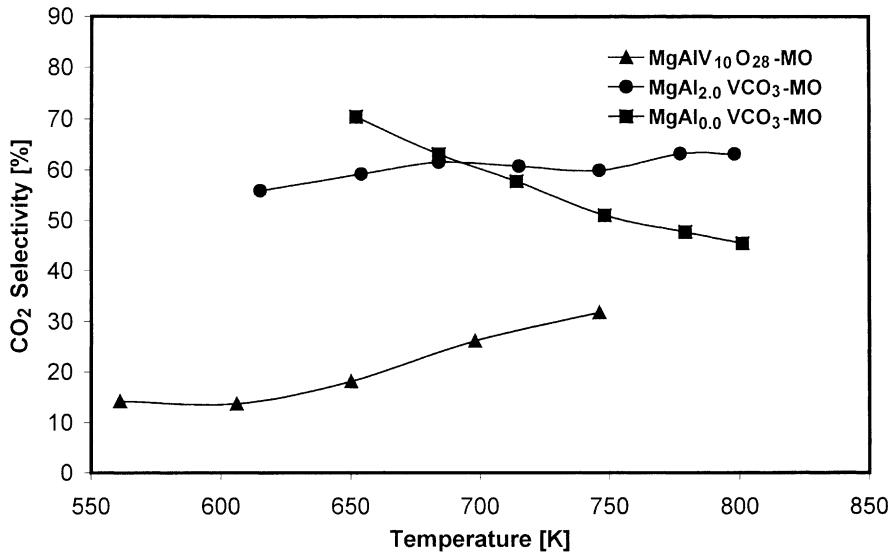

Fig. 5. Temperature dependence of selectivity to CO_2.

CO is formed mainly by consecutive combustion of propene, whereas CO_2 stems chiefly from the parallel process of total combustion of propane [3,35,38–40]. Thus, it appears that the parallel combustion of C_3H_8 to CO_2 is much more pronounced on the catalysts obtained from the layer-doped precursors than on the catalyst derived from the LDH containing decavanadate in the interlayer.

The differences in the catalytic performance are particularly striking when one compares the $MgAlV_{10}O_{28}$-MO and $MgAl_{0.0}VCO_3$-MO samples, characterised by similar total V content, similar

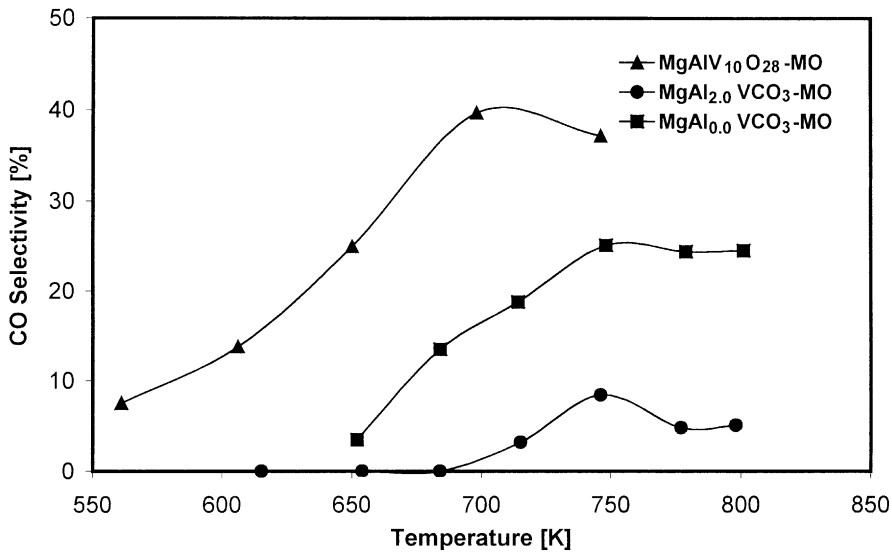

Fig. 6. Temperature dependence of selectivity to CO.

surface density of V centres, and similar specific surface areas. A natural conclusion is the assumption that the surface V centres present in both materials possess different intrinsic activity/selectivity characteristics. This conclusion is compatible with the results of ESR characterisation, which detected a difference in the covalency of in-plane V(IV)–O π-bonds present in both samples, and with the XRD data pointing to the different nature of magnesium vanadates. The pyrovanadate phase nucleating at the surface of $MgAlV_{10}O_{28}$-MO is known to be more reducible than the *ortho*-vanadate present in $MgAl_{0.0}VCO_3$-MO [40,41]. This accounts for the higher degree of propane conversion over this material, because in the oxidation reactions proceeding via Mars van Krevelen redox mechanism, the liability of surface oxide ions is directly related to the catalyst activity. The direct correlation between the total activity in the ODH reactions and the reducibility of vanadium catalysts was in fact reported previously [41,42]. The observed selectivity patterns, pointing to the more selective nature of $MgAlV_{10}O_{28}$-MO when compared to $MgAl_{0.00}VCO_3$-MO, may be discussed, following the reasoning of one of the present authors [43], in terms of the differences in the character of surface V sites and the nature of surface oxygen species. Re-oxidation of vanadia-based catalysts involves chemisorption of an oxygen molecule and its dissociation with the electron extraction from the solid, according to the following scheme:

$$O_2 \xrightarrow{e^-} O_2^- \xrightarrow{e^-} 2O^- \xrightarrow{2e^-} 2O^{2-}$$

The electrophilic oxygen radicals O_2^- and O^- favour total oxidation of hydrocarbons [44]. In order to avoid an attack of these species on a hydrocarbon molecule and obtain high selectivity to partial oxidation products, the subsequent transformation of O_2^- and O^- to nucleophilic O^{2-} species should be possibly fast. The latter process will be the more efficient the higher is the availability of electrons derived from the reduced vanadium ions. Thus, the isolation of the V centres, such as that imposed by the crystal structure of *ortho*-vanadate, and the lower reducibility of this compound would favour the presence of electrophilic oxygen species and, consequently, total oxidation rather than the selective pathway. On the other hand, dimeric vanadium units present in the more reducible pyrovanadate phase provide the necessary conditions for the formation of nucleophilic oxygen species, thus, suppressing the total oxidation of propane. The observed higher selectivities to propene over $MgAlV_{10}O_{28}$-MO, especially in the lower temperature range, are consistent with the above reasoning.

In view of the presented results, it seems logical to associate the higher activity and selectivity in ODH of propane of the mixed oxide sample derived from the LDH material containing decavanadate in the interlayer with nucleation of the magnesium pyrovanadate phase. On the other hand, the appearance of the magnesium *ortho*-vanadate observed in catalyst obtained from layer-doped precursor, seems to have an adverse effect on the catalytic properties. The observation supports the earlier conclusions of Volta and co-workers [3] attributing the good activity and selectivity of V-Mg-O catalysts in ODH of propane to the presence of magnesium pyrovanadate. The specific features of this phase such as higher reducibility [6,40,41], the ability to stabilise V(IV) sites associated with the surface oxygen vacancies [40] and the limited lattice oxygen exchange with the gas phase [45] have been listed as factors determining its superior properties in ODH of propane. Our studies add the electronic structure of reduced vanadium ions as yet another specificity of magnesium pyrovanadate phase.

Comparison of the trends in selectivities to various reaction products on two catalysts derived from layer-doped precursors shows that the selectivity to propene is higher on the $MgAl_{2.0}VCO_3$-MO sample, containing aluminium, than on the aluminium-free $MgAl_{0.0}VCO_3$-MO one. The result is different from the finding of Blasco and López Nieto, who examined the catalytic performance of vanadium V/MgO and V/Mg-Al-O systems in ODH of alkanes [42] and found that the presence of aluminium resulted in a lower selectivity to olefin. The authors argued that addition of aluminium rendered the catalyst surface more acidic and capable of stronger interaction with the basic olefin molecule, lowering in consequence its desorption rate. Obviously, in the present case, some other factor must play a more important role. One of the possibilities could be the different degree of crystallisation of the V-containing phases. In the $MgAl_{0.0}VCO_3$-MO sample, magnesium *ortho*-vanadate has been identified by XRD, while in the $MgAl_{2.0}VCO_3$-MO catalyst the V-containing phase remained amorphous. It is conceivable that the

degree of long range ordering might affect the properties of the individual V sites. Indeed, the ESR study reveals not only similarity between the paramagnetic V centres present in both materials, such as the degree of covalency of in-plane bonds, but also differences manifested in small changes of bond lengths around the respective sites.

4. Conclusions

Catalytic performance of samples derived from V-containing LDHs depends on the manner of incorporation of the vanadium dopant into the LDH structure. The catalyst obtained from interlayer-doped precursor is more active and selective than the materials derived from the LDH containing vanadium in the brucite layer. The lower selectivity to propene on the catalysts obtained from the layer-doped precursors is associated with the more pronounced tendency for direct combustion of propane to CO_2. The observed effects are attributed to the different nature of magnesium vanadates nucleating in the mixed oxides obtained by calcination of differently doped LDH precursors: pyrovanadate in the case of interlayer- and *ortho*-vanadate in the case of layer-doping. It is argued that in the former V centres of higher intrinsic activity and selectivity are formed. These properties could be due to the lower covalency of V–O bonds, as indicated by the electronic structure of the paramagnetic vanadium defects seen by ESR. Different degree of crystallinity of V-containing phases is tentatively proposed as a possible reason for differences in the catalytic properties of two materials obtained from layer-doped precursors.

Acknowledgements

This work was supported in part by the Polish Committee for Scientific Research, within the project no. 3-T09A-017-15.

References

[1] E.A. Mamedov, V. Cortés Corberán, Appl. Catal. A 127 (1995) 1–40.
[2] M.A. Chaar, D. Patel, H.H. Kung, J. Catal. 109 (1988) 463.
[3] D. Siew Hew Sam, V. Soenen, J.C. Volta, J. Catal. 123 (1990) 417.
[4] P.M. Michalkos, M.C. Kung, I. Jahan, H.H. Kung, J. Catal. 140 (1993) 226.
[5] A. Corma, J.M. López Nieto, N. Paredes, J. Catal. 144 (1993) 425.
[6] X. Gao, P. Ruiz, Q. Xin, X. Guo, B. Delmon, J. Catal. 148 (1994) 56.
[7] S.R.G. Carrazán, C. Peres, J.P. Bernard, M. Ruwet, P. Ruiz, B. Delmon, J. Catal. 158 (1996) 452.
[8] A. Pantazidis, A. Auroux, J.-M. Herrmann, C. Mirodatos, Catal. Today 32 (1996) 81.
[9] D.L. Stern, J.N. Michaels, L. DeCaul, R.K. Grasselli, Appl. Catal. A 153 (1997) 21.
[10] H.H. Kung, M.C. Kung, Appl. Catal. A 157 (1997) 105.
[11] J.M. López Nieto, A. Dejoz, M.I. Vasquez, W. O'Leary, J. Cunningham, Catal. Today 40 (1998) 215.
[12] J.M. López Nieto, J. Soler, P. Concepción, J. Herguido, M. Menédez, J. Santamariá, J. Catal. 185 (1999) 324.
[13] R.X. Valenzuela, V. Cortés Corberán, Topics Catal. 11 (2000) 153.
[14] K. Bahranowski, G. Bueno, V. Cortés Corberán, F. Kooli, E.M. Serwicka, R.X. Valenzuela, K. Wcisło, Appl. Catal. A 185 (1999) 65.
[15] F. Cavani, F. Trifiró, A. Vaccari, Catal. Today 11 (1991) 173.
[16] V. Rives, F.M. Labajos, M.A. Ulibarri, P. Malet, Inorg. Chem. 32 (1993) 5000.
[17] F.M. Labajos, V. Rives, P. Malet, M.A. Centeno, M. Ulibarri, Inorg. Chem. 35 (1996) 1154.
[18] F. Kooli, I. Crespo, C. Barriga, M.A. Ulibarri, V. Rives, J. Mater. Chem. 6 (1996) 1199.
[19] C.H. Baes, R.E. Mesner, The Hydrolysis of Cations, Wiley, New York, 1967.
[20] C.D. Wagner, W.M. Riggs, L.E. Davis, J.F. Moulder, G.E. Mullenberg, Handbook of X-ray Photoelectron Spectroscopy, Perkin-Elmer, Physical Electronics Division, Eden Prairie, MN, 1979.
[21] A. Abragam, B. Bleaney, Electron Paramagnetic Resonance of Transition Ions, Oxford University Press, Oxford, 1970.
[22] L.D. Rollmann, S.I. Chan, J. Chem. Phys. 50 (1969) 3416.
[23] R. Aasa, T. Vangard, J. Magn. Reson. 19 (1975) 320.
[24] E.M. Serwicka, Crit. Rev. Surf. Chem. 1 (1990) 27.
[25] M.A. Drezdzon, Inorg. Chem. 27 (1988) 4628.
[26] E. Narita, P. Kaviratna, T.J. Pinnavaia, Chem. Lett. 5 (1991) 805.
[27] E. Lopez Salinas, Y. Ono, Bull. Chem. Soc. Jpn. 65 (1992) 2465.
[28] M.A. Ulibarri, F.M. Labajos, V. Rives, R. Trujillano, W. Kagunya, W. Jones, Inorg. Chem. 33 (1992) 2592.
[29] J. Wang, Y. Tian, R.-C. Wang, A. Clearfield, Chem. Mater. 4 (1992) 1276.
[30] G.L.M. Clarck, R. Morley, J. Solid State Chem. 16 (1976) 429.
[31] J. Twu, P.K. Dutta, J. Catal. 124 (1990) 503.
[32] K. Bahranowski, R. Dula, F. Kooli, E.M. Serwicka, Colloids Surf. A 158 (1999) 129.

[33] V.K. Sharma, A. Wokaun, A. Baiker, J. Phys. Chem. 90 (1986) 2715.
[34] J.G. Eon, R. Olier, J.C. Volta, J. Catal. 145 (1994) 318.
[35] R. Grabowski, B. Grzybowska, K. Samson, J. Słoczyński, J. Stoch, K. Wcisło, Appl. Catal. A 125 (1995) 129.
[36] G. Centi, F. Trifiró, Appl. Catal. A 143 (1996) 3.
[37] J.N. Michaels, D.L. Stern, R.K. Grasselli, Catal. Lett. 42 (1996) 135.
[38] A. Corma, J.M. López Nieto, N. Paredes, M. Pérez, Appl. Catal. A 97 (1993) 159.
[39] P. Viparelli, P. Ciambelli, L. Lisi, G. Ruoppolo, G. Russo, J.C. Volta, Appl. Catal. A 184 (1999) 291.
[40] A. Guerrero-Ruiz, I. Rodríguez-Ramos, J.L.G. Fierro, V. Soenen, J.M. Herrmann, J.C. Volta, in: P. Ruiz, B. Delmon (Eds.), Studies in Surface Science and Catalysis, Vol. 72, Elsevier, Amsterdam, 1992, p. 203.
[41] V. Soenen, J.M. Herrmann, J.C. Volta, J. Catal. 159 (1996) 410.
[42] T. Blasco, J.M. López Nieto, Appl. Catal. A 157 (1997) 117.
[43] B. Grzybowska-Świerkosz, Appl. Catal. A 157 (1997) 409.
[44] A. Bielański, J. Haber, Catal. Rev.-Sci. Eng. 19 (1979) 1.
[45] A. Guerrero-Ruiz, I. Rodríguez-Ramos, P. Ferreira-Aparicio, J.C. Volta, Catal. Lett. 45 (1997) 113.